

UDK: 661.728.7; 534.12; 549.791.1; 543.393

## Evaluation of Adsorption Performance and Quantum Chemical Modeling of Pesticides Removal using Cell-MG Hybrid Adsorbent

Jovana Perendija<sup>1</sup>, Zlate S. Veličković<sup>2</sup>, Ljubinka Dražević<sup>3</sup>, Ivana Stojiljković<sup>4</sup>, Miloš Milčić<sup>5</sup>, Milutin M. Milosavljević<sup>3</sup>, Aleksandar D. Marinković<sup>6\*)</sup>, Vladimir Pavlović<sup>7,8</sup>

<sup>1</sup>University of Belgrade, Institute of Chemistry, Technology and Metallurgy, National Institute of the Republic of Serbia, Njegoševa 12, 11001 Belgrade, Serbia

<sup>2</sup>Military Academy, University of Defense, Veljka Lukića Kurjaka 33, 11000 Belgrade, Serbia

<sup>3</sup>Faculty of Technical Science, University of Priština, Str. Knjaza Miloša 7, 38220 Kosovska Mitrovica

<sup>4</sup>Faculty of Forestry, University of Belgrade, Kneza Višeslava 1, 11030 Beograd, Serbia

<sup>5</sup>Faculty of Chemistry, University of Belgrade, Studentski trg 12-16, 11158 Beograd, Serbia

<sup>6</sup>Faculty of Technology and Metallurgy, University of Belgrade, Karnegijeva 4, 11060 Belgrade, Serbia

<sup>7</sup>Institute of Technical Sciences of SASA, 11000 Belgrade, Serbia

<sup>8</sup>Faculty of Agriculture, University of Belgrade, 11000 Belgrade, Serbia,

---

### Abstract:

*Magnetite (MG) modified cellulose membrane (Cell-MG), obtained by reaction of 3-aminosilane and subsequently with diethylenetriaminepentaacetic acid dianhydride functionalized waste Cell fibers (Cell-NH<sub>2</sub> and Cell-DTPA, respectively), and amino-modified diatomite was used for Azoxystrobin and Iprodione removal from water. Cell-MG membrane was structurally and morphologically characterized using FT-IR and FE-SEM techniques. The influences of operational parameters, i.e. pH, contact time, temperature, and the mass of adsorbent on adsorption and kinetics were studied in a batch system. The calculated capacities of 35.32 and 30.16 mg g<sup>-1</sup> for Azoxystrobin and Iprodione, respectively, were obtained from non-linear Langmuir model fitting. Weber-Morris model fitting indicates the main contribution of intra-particle diffusion to overall mass transport resistance. Thermodynamic data indicate spontaneous and endothermic adsorption. The reusability of adsorbent and results from wastewater purification showed that Cell-MG could be used as general-purpose adsorbent. The adsorbent/adsorbate surface interaction was considered from the results obtained using density functional theory (DFT) and calculation of molecular electrostatic potential (MEP). Thus, a better understanding of the relation between the adsorption performances and contribution of non-specific and specific interactions to adsorption performances and design of novel adsorbent with improved properties was deduced.*

**Keywords:** Cellulose membrane; Magnetite; Pesticide; Quantum-chemical calculations.

---

\*) Corresponding author: marinko@tmf.bg.ac.rs

## 1. Introduction

Aquatic environmental pollutions due to the presence of heavy metal ions and toxic organic compounds in wastewater, is a major environmental concern. Heavy metals are serious chemical pollutants because of their persistence in the environment, toxicity, and bioaccumulation. Hence, there is a requirement to remove their traces from the effluent [1]. In the modern-day intensive agricultural industry, the use of pesticides is unavoidable and very common, in order to optimize the food protection process required by the growing human population. Approximately, 2 million tonnes of pesticides are spending annually worldwide, and in the 2020 year, global pesticide usage has been estimated to increase up to 3.5 million tonnes [2]. A small percentage of applied pesticides reach the target organism and it is considered that all residues entering waters and soils. Aquatic pollution caused by pesticides as a consequence of run-off, leaching, and sub-surface drainage, may pose a serious health hazard for living being and ecosystems due to pesticides persistent nature and bio-magnification [3]. Since most organic pesticides are non-degradable and carcinogenic, they represent a potent category of water contaminants.

Iprodione is an imidazole fungicide commonly used as a contact pesticide against fungal pathogens in plants [4]. It is considered to be moderately toxic to small animals and probable carcinogen to humans [5]. Iprodione's relatively low *K<sub>oc</sub>* signify rather a weak sorption to soil pointing to a potential for relatively high mobility in soil. Researches are indicated the presence of iprodione and its metabolites in surface and drainage water [5].

Azoxystrobin is a systemic broad-spectrum fungicide approved for use on more than 80 different crops. It is considered to be mobile in the environment because he is water-soluble and slow to degrade in soil and water [3]. Azoxystrobin has been shown to be moderate to highly toxic to aquatic organisms [6].

Heavy metal ions and organic pollutants removal from wastewater may be achieved by chemical and physical treatment and the goal is to implement cheaper and more efficient technology. However, most remediation treatments have a high cost, lower efficacy, limited flexibility and possible secondary contaminant production. The adsorption process onto low-cost materials is distinguished as a promising technique to remove pollutants from aqueous solution. Adsorption is an effective process of wastewater treatment due to its high efficiency, cost-effectiveness, easy handling as well due to the use of sorbents that are abundant [7,8]. Industries often apply adsorption to diminish hazardous toxic ions and organic contaminants present in the effluent [3].

Cellulose is the abundant natural raw material, which is renewable, fibrous, tough and water-insoluble polymer. It is harmless to the environment because of the safe return to the natural carbon cycle, within a simple decay process in the presence of decomposers. Cellulose shows potential as a sorbent, due to its non-toxicity, facile chemical modification, favourable mechanical properties, and safe disposal after use [9]. A significant amount of a renewable and biodegradable raw material available from different sources may be utilized as a sorbent in various forms such as raw cellulose or modified cellulose, to eliminate pollutants from water. Raw cellulose can be utilized as an adsorbent but owing to its low adsorption capacity, chemical modification is preferred to achieve an effective removal of contaminants [9]. Cellulose undoubtedly has a huge potential to develop into an effective adsorbent for water treatment.

Diatomite (D) has received great attention since it has unique advantages as an adsorbent, *i.e.*, high porosity, high permeability, small particle size, large surface area, low thermal conductivity and chemical inertness. The simultaneous introduction of waste cellulose and diatomite into an adsorbent polymeric networks has performed with the aim of developing eco-friendly materials for wastewater treatment [10].

It is a well-known fact that iron oxides, such as magnetite and hematite, are very successful in cations and oxyanions removal, but their effectiveness in removing pesticides

has yet to be examined. Synthesis techniques of iron oxides include hydrolysis of acidic solutions of Fe<sup>III</sup> salts, the transformation of ferrihydrite, oxidative hydrolysis of Fe<sup>II</sup> salts, phase transformations, gel-sol method, decomposition of metal chelates and hydrothermal precipitation [11,12]

The implementation of the waste cellulose with diatomite, as adsorbent material is improved when he has a magnetic response since the magnetized form of the material allows a more natural separation of the adsorbent from treated water a direct application of a magnetic field. Magnetite particles have attracted major attention because of their many potential applications. However, magnetite also has some limitations, such as a lack of molecular selectivity, aggregation and low binding capacity. A simple solution to overcome these disadvantages is the deposition of magnetite particles on the polymer surface [13]. Hence, this study has researched the feasibility of using magnetic bio-material as a low-cost adsorbent for heavy metal ions and organic compounds removal [14,15].

Competitive adsorption is the common occurrence in practice since the wastewaters to be treated are multicomponent mixtures, hence it is of critical importance in determining the overall performance of an adsorbent. The presence of other organic or inorganic substances in water influence the efficacy of the tested adsorbent consequently the objective of the present study was to examine the mutual effects of metal ions and pesticides in a multicomponent system on adsorbent performance.

The aim of this study was further use of previously developed cost-effective Cell-MG membrane [16] for the removal of Azoxystrobin and Iprodione pesticides. Also, Cell membrane obtained by wet dipping of Cellulose modified with 3-aminopropyltriethoxysilane (Cell-NH<sub>2</sub>) in first step and further modified with diethylenetriaminepentaacetic acid dianhydride (Cell-DTPA) with magnetite and hematite was comparatively used for pesticide removal. After selection Cell-MG membrane the objectives of the presented study was the determination of i) adsorption capacity, ii) thermodynamic parameters, iii) kinetic and activation parameter determination, iv) and quantum chemical calculations as a useful method applied for the description of adsorption mechanism.

## **2. Materials and Experimental Procedures**

### **2.1 Cell-MG hybrid membrane preparation**

Cell-MG hybrid membrane and D-APTES (Diatomite modified with 3-aminopropylsilane, i.e. APTES) was prepared following procedure described by Perendija *et al.* [16]. Magnetite and hematite was also synthesized according to the method described in literature [11]. Cell-DTPA membrane was loaded with magnetite and hematite using ultrasonication and wet dipping method.

### **2.2 Characterization of adsorbents**

Full details on characterization methods are given in Supplementary material.

### **2.3 Batch adsorption experiments**

Adsorption experiments, performed in a batch system, related to adsorption and kinetic study, are presented in Supplementary material.

### **2.4 Regeneration study**

Regeneration method is provided in Supplementary material.

## 2.5 Computational detail

The initial structure of azoxystrobin was taken from Cambridge Structural Database (CSD) (Refcode DIZVAM [17]) and initial structure of iprodione was constructed as z-matrix. Both structures were subjected to extended conformational search followed by geometry optimization with B3LYP hybrid functional and 6-31(d,p) basis set in order to find global minima conformers. Next, lowest energy conformers are re-optimized with B3LYP/6-311G(d,p) method, and these structures are used for further investigation. All quantum chemical calculations were done with Gaussian 09 (revision D.01) program [18].

Multiwfn [19] program (version 3.6) was used for analyzing calculated electrostatic potential on molecular surface [20]. The colour mapped isosurface graphs of electrostatic potential (ESP) mapped on van der Waals (vdW) molecular surface (electron density of  $0.001 \text{ e}/\text{\AA}^3$ ) were produced in VMD 1.9.3. program [21].

The molecular interaction field indices (MIF) were calculated in Open3DQSAR program [22] using vdW and electrostatic potential from quantum chemical calculations. The HOH probe was used for calculating hydrogen bond donor part of the molecule and NR probe was used for calculating hydrogen bond acceptor part of the molecule. In the MIF graphs, only areas with interaction energy between molecule and probe higher than 5 kcal/mol are shown.

## 3. Results and Discussion

### 3.1. Synthesis of iron oxides loaded Cell membrane

Previously synthesized Cell-MG membrane [16] was used in a study of Azoxystrobin and Iprodione removal to evidence its value in a process of organic pollutants from water. Also, two comparative material, i.e. magnetite and hematite, was prepared according the literature method [11]. Cellulose modified with 3-aminopropyltriethoxysilane (Cell-NH<sub>2</sub>) and further modified with diethylenetriaminepentaacetic acid dianhydride (Cell-DTPA) [16] was loaded with magnetite and hematite to produce Cell-MG(d) and Cell-hematite(d) membrane. Preliminary adsorption study showed lower adsorption capacity of Cell-MG(d) and Cell-hematite(d) for 21 % and 44 %, respectively. Except of this, low stability due to physical adsorption, i.e. loosely bonded magnetite and hematite to Cell-DTPA surface, decrease working life due to their release in a water solution in the course of adsorption and thus lower performances is a consequence. According to that it was confirmed importance of the controlled precipitation magnetite on Cell-DTPA, i.e. formation of covalently bonded crystallization centre, to obtain improved performances and working life of adsorbent. Thus, Cell-MG hybrid membrane was selected for further adsorption study.

### 3.2. Characterization of the Cell-MG hybrid adsorbent after adsorption

#### 3.2.1 FTIR spectroscopy

FTIR technique was used to monitor the changes of Cell-MG hybrid membrane structure after adsorption experiments. FTIR spectra of Cell-MG hybrid membrane previously was characterized by Perendija *et al.* [16]. In the Cell-MG adsorbent spectrum (Fig. 1), the strong adsorption at  $3430 \text{ cm}^{-1}$  occurs as a result of the stretching of the O-H, bonded water and Fe-OH surface groups. The vibrational band at  $2922$  and  $2853 \text{ cm}^{-1}$  is due to the valence of C-H stretching vibration [23]. The region from  $1640$ - $1384 \text{ cm}^{-1}$  is attributed to the bending mode of OH and C-H groups derived from cellulose. A broad band centered at  $1090 \text{ cm}^{-1}$  indicates the presence of Si-O-Si from diatomite and with a major contribution of C-O groups

in a cellulose polysaccharide skeleton [24]. The signal at  $574\text{ cm}^{-1}$  corresponds to stretching vibrations of the Fe–O bond [25,26].

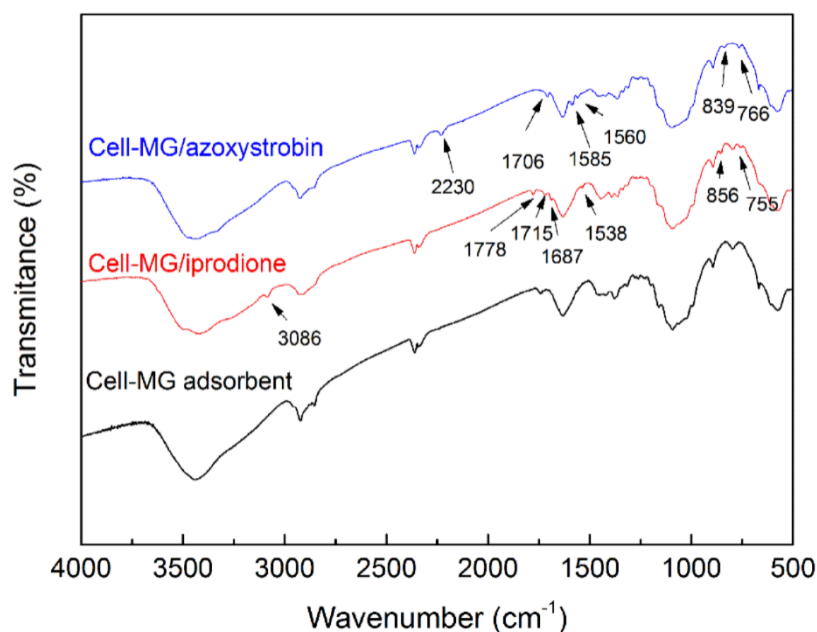


**Fig. 1.** FTIR spectra of Cell-MG membrane before and after Iprodione (Cell-MG/iprodione) and Azoxystrobin adsorption (Cell-MG/azoxystrobin).

There is observable change in the spectrum Cell-MG/Azoxystrobin obtained after pesticide adsorption. The peak at  $2230\text{ cm}^{-1}$  is due to cyano group stretching vibration, while a small peak at  $1706\text{ cm}^{-1}$  is assigned to conjugated carbonyl ester vibration. Two observable peaks at  $1585$  and  $1560\text{ cm}^{-1}$  are due to the skeletal stretching vibration of phenyl and pyrimidine rings. Additionally, two peaks at  $839$  and  $766\text{ cm}^{-1}$  are related to deformation out-of-plane vibration of substituted aromatic rings.

Similarly, after Iprodione adsorption, new bands on the FTIR spectra in the range of  $1738$ – $888\text{ cm}^{-1}$  were observed. The intense band at  $1715$  and  $1687\text{ cm}^{-1}$  is attributed to carbonyl stretch vibration presents in amide groups. The weak intensity peak at  $1538\text{ cm}^{-1}$  belongs to symmetric stretching vibrations of the C=C group in the aromatic ring skeleton. The weak band located at  $1445\text{ cm}^{-1}$  can be attributed to the pseudo symmetric N–C=O stretching in imidazolodine-2,4-dione ring which is a part of the Iprodione molecule[27]. The peak at  $1363\text{ cm}^{-1}$  belongs to the deformation vibration of the isopropyl part. The expected band in the region  $1000$ – $1100\text{ cm}^{-1}$  from stretching vibration of C–Cl bond linked to the aromatic ring is overlapped with C–O vibration from cellulose [28].

### 3.2.2 Surface Morphology analysis

The results from morphology analyses of the Cell-MG membrane and one loaded with MG nanoparticles, using SEM and TEM techniques, respectively, are given in Fig. 2. Also SEM micrograph of D and D-APTES is given on Fig. S2.

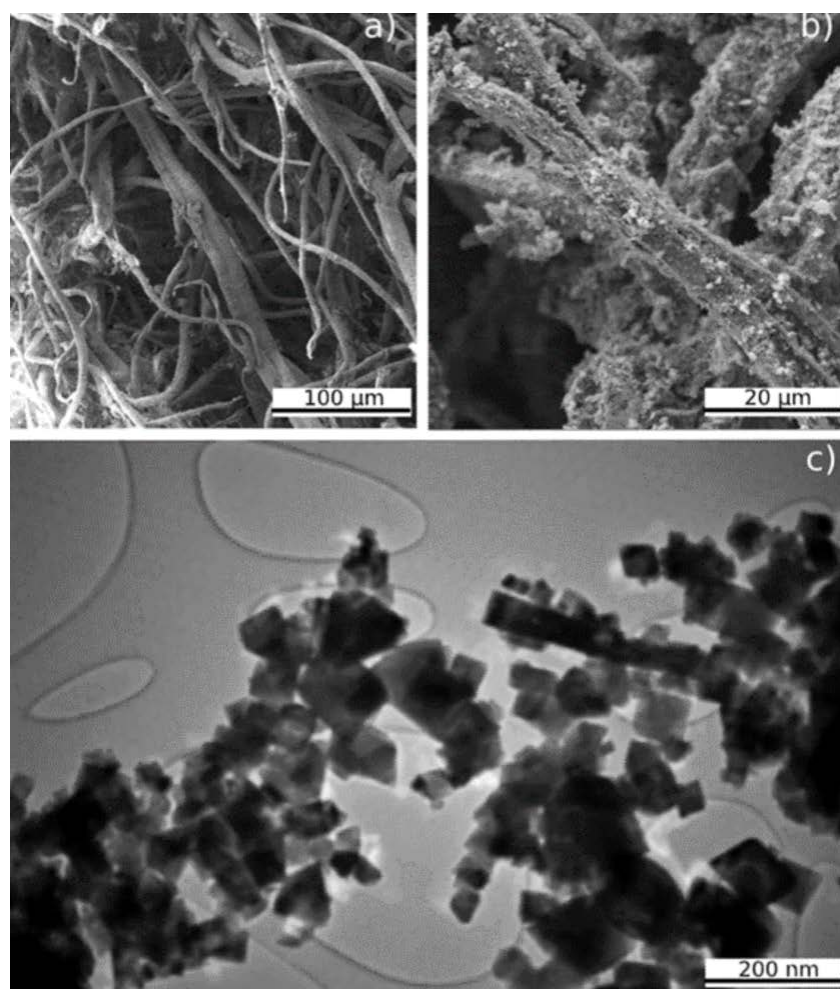


**Fig. 2.** SEM images of Cell based membrane (a) and Cell-MG hybrid membrane (b) and c) TEM image of Fe<sub>3</sub>O<sub>4</sub> particles.

Applied optimized procedure, used for precipitation of MG on Cell-COOH membrane, provides uniform distribution of MG nanoparticles contributing to increase of adsorbent surface and Fe-OH active site able to perform pollutant removal. No change in the structure of the cellulosic fibres was observed, while the surface morphology of the hybrid adsorbent significantly changed due to MG precipitation. It was shown that 7.8 wt.% of iron, i.e. ~10.8 wt.% of MG of evenly distributed MG nanoparticle was loaded in Cell-MG hybrid membrane [16].

### 3.3. Adsorption study

#### 3.3.1 Adsorption isotherms modeling

The adsorption capacities were determined from equilibrium data at optimal operational pH 6. The equilibrium adsorption data were fitted with the four isotherm models: Langmuir Eq. (S3), Freundlich Eq. (S4), Dubinin–Radushkevich Eq. (S6) and Temkin Eq. (S7), and obtained results is given in Tables I and II.

**Tab. I** The results of non-linear fitting using Langmuir isotherm model for azoxystrobin and iprodione adsorption onto Cell-MG hybrid membrane.

Langmuir model		$q_m$ (mg g <sup>-1</sup> )	$K$ (dm <sup>3</sup> mg <sup>-1</sup> )	$K_L$ (dm <sup>3</sup> mol <sup>-1</sup> )	$R^2$
Azoxystrobin	25 °C	35.32	3.46	1396381.2	0.976
	35 °C	35.67	3.75	1514582.5	0.976
	45 °C	35.99	4.10	1656081.5	0.976
Iprodione	25 °C	30.16	4.59	1515080.2	0.986
	35 °C	30.44	5.56	1837412.1	0.989
	45 °C	30.66	7.09	2317366.2	0.992

**Tab. II** Non-linear Freundlich, Temkin and Dubinin-Radushkevich isotherm parameters for azoxystrobin adsorption on Cell-MG membrane.

		Parameters	25 °C	35 °C	45 °C
Freundlich isotherm		$K_F$ (mg g <sup>-1</sup> )(dm <sup>3</sup> mg <sup>-1</sup> ) <sup>1/n</sup>	23.54	24.13	24.65
		$1/n$	0.387	0.375	0.361
		$R^2$	0.993	0.993	0.991
Temkin isotherm		$A_T$ (dm <sup>3</sup> g <sup>-1</sup> )	70.44	84.13	105.68
		$b_T$	438.6	463.33	494.81
		$B$ (mg g <sup>-1</sup> )	5.65	5.53	5.35
		$R^2$	0.939	0.931	0.918
Dubinin-Radushkevich isotherm		$q_m$ (mg g <sup>-1</sup> )	22.05	21.94	21.67
		$K_{ad}$ (mol <sup>2</sup> KJ <sup>-2</sup> )	9.81	9.82	9.83
		$E_a$ (KJmol <sup>-1</sup> )	7.138	7.136	7.131
		$R^2$	0.863	0.847	0.825

**Tab. III** Non-linear Freundlich, Temkin and Dubinin-Radushkevich isotherm parameters for iprodione adsorption on Cell-MG membrane.

		Parameters	25 °C	35 °C	45 °C
Freundlich isotherm		$K_F$ (mg g <sup>-1</sup> )(dm <sup>3</sup> mg <sup>-1</sup> ) <sup>1/n</sup>	23.06	24.32	25.61
		$1/n$	0.386	0.374	0.356
		$R^2$	0.995	0.993	0.991
Temkin isotherm		$A_T$ (dm <sup>3</sup> g <sup>-1</sup> )	102.32	132.07	185.81
		$b_T$	512.83	538.04	572.76
		$B$ (mg g <sup>-1</sup> )	4.83	4.76	4.62
		$R^2$	0.957	0.960	0.961
Dubinin-Radushkevich isotherm		$q_m$ (mg g <sup>-1</sup> )	20.40	21.01	21.53
		$K_{ad}$ (mol <sup>2</sup> KJ <sup>-2</sup> )	9.69	9.66	9.64
		$E_a$ (KJmol <sup>-1</sup> )	7.183	7.193	7.202
		$R^2$	0.915	0.920	0.921

Moderate adsorption capacities ( $q_m$ ), obtained using Langmuir isotherm model (Table I), is almost constant at all temperature which indicate physical type of pesticide bonding. Also, high values of the Langmuir constant ( $K_L$ ) reflect the pronounced sorption affinity of the sorbate toward adsorbent surface. It means that adsorption produced is induced by high adsorbent surface affinity to pesticides by creating weak interaction with surface functionalities.

As it can be seen from Tables II and III, the Freundlich isotherm is the best fitting model used for description of adsorption equilibrium. The obtained parameter  $n$  were in the range of 1-10, indicating a favourable adsorption process ( $R_L$ , calculated according to Eq. (S5), are in the range from 0.024 to 0.224 for Azoxystrobin; Iprodione from 0.013 to 0.163). Additional evidence of good adsorption capacity is constant  $K_F$ , as an approximate indicator of adsorption capacity, showed also analogous trend (Table I).

### 3.3.2 Thermodynamic parameters of adsorption

The Gibbs free energy ( $\Delta G^\ominus$ ), enthalpy ( $\Delta H^\ominus$ ) and entropy ( $\Delta S^\ominus$ ) calculated from Van't Hoff equation (Eqs. (S8) - (S10)) are given in Tab. IV, and used for the analysis of thermodynamic aspect of the adsorption.

**Tab. IV** Calculated Gibbs free energy, enthalpy and entropy for the Azoxystrobin and Iprodione adsorption on Cell-MG hybrid membrane.

Pesticide	$\Delta G^\ominus$ (kJ mol <sup>-1</sup> )			$\Delta H^\ominus$ (kJ mol <sup>-1</sup> )	$\Delta S^\ominus$ (J mol <sup>-1</sup> K <sup>-1</sup> )	R <sup>2</sup>
	298 K	308 K	318 K			
Azoxystrobin	-45.03	-46.75	-48.50	6.72	173.55	0.998
Iprodione	-40.95	-42.82	-44.82	16.73	193.4	0.995

The  $\Delta H^\ominus$  values reflect the energetic effect of the overall process and describe the contribution of elemental processes such as: endothermicity of the desolvation of pesticide, i.e. breakage of the intermolecular solute-solvent interactions, diffusional processes and exothermicity of pesticide-surface functionalities interactions. Different type and low intensity electrostatic/hydrogen bonding interaction request and involvement of energy to perform desolvation, where the strength of the interaction is highly affected by electronic density distribution over investigated pesticide (see subchapter 3.6). The overall energy change indicates that liberated energy from formation surface interaction slightly exceeds the energy liberated by the adsorbent surface interactions, and thus low positive  $\Delta H^\ominus$  is a consequence. The higher value of  $\Delta H^\ominus$  for Iprodione indicate that higher dipolarity of present functionalities and lower voluminosity provides an easier approach to surface followed by stronger interactions.

The gradual  $\Delta G^\ominus$  increase *versus* the temperature increase means more favourable desolvation and diffusional processes at a higher temperature. According to literature for  $\Delta G^\ominus$  in the range, -20 and 0 kJ mol<sup>-1</sup> physisorption dominate, -20 to -80 kJ mol<sup>-1</sup> both physisorption and chemisorption participate, and -80 and -200 kJ mol<sup>-1</sup> chemisorption prevail [29]. Thus, from obtained results, i.e. the  $\Delta G^\ominus$  values in the range -45.03 to -49.66 kJ mol<sup>-1</sup>, clearly indicate spontaneous process with the participation of both physisorption and chemisorption processes.

The high  $\Delta S^\ominus$  indicates increased randomness at the adsorbent/solution interface. Different arrangement and orderliness of solvated pesticides, considering the type and extent of intermolecular interactions, and hydration of surface functionalities contribute to the change of the freedom of the local system in the course of adsorption. The progress of the adsorption process is accompanied by the formation of surface structure with the adsorbed pesticide by forming different interactions. These interactions are strongly influenced by molecular structure, i.e. spatial arrangement adopted to achieve optimal interactions with surface functionalities, and properties of surface functional groups (see subchapter 3.6). Concomitantly with pesticide approach/bonding water release take place predominantly or desorption of other exchangeable ion. Thus entropy change of elementary processes contributes to the  $\Delta S^\ominus$  value change of the adsorption process.



### 3.3.3 Desorption study

Nowadays, numerous studies dealing with the development of effective adsorbents for pesticide removal from water, but less attention is paid to the regeneration process. The regeneration process is crucial to improve the function and capacity of the adsorbent used, and the reuse of the adsorbent is required in order to make the adsorption process environmentally admissible and economic. Hence, the selection of appropriate desorption method with re-utilization of the adsorbents in adsorption-desorption cycles could help to resolve this important issue. The overall desorption efficiency and the number of adsorption-desorption cycles decrease with a partial influence of several factors which impair adsorbent performance (i.e. incomplete desorption, precipitation and pore-clogging, destruction of active sites etc.). The disposal of adsorbent may generate a problem in the environment following the continuous accumulation of pesticides on the adsorbents and also affects the environment due to the potential leaching of the adsorbate. Regeneration of adsorbents is a challenge because using a proper technique helps in improving adsorption efficiency by removing pesticides, decrease the overall cost of the treatment process, reduces the generated waste and solves the disposal problem. The choice of desorbing agent depends on the kind of adsorbent used and the pesticides adsorbed. An effective desorbing agent is one that desorbs the pesticide entirely without degradation of the properties of the adsorbent. In the present study, a number of various alkaline and acidic desorbing agents were investigated and it was concluded that their performance strongly depended on the bonding types as well as strength between adsorbate and surface functionalities.

Optimization of the desorption procedure, using Cell-MG hybrid membrane, was performed with respect to concentration and type of regenerating agent used (Supplementary material). Many factor influences decision on the efficacy of wastewater treatment technology: adsorption and desorption efficiency, work-life of the adsorbent and technology applied for generated waste (effluent water solution after desorption). Pesticide desorption increases with both pH increase and decreases, whereby the use of  $\text{NaHCO}_3$  and  $\text{NaOH}$  provided >95% pesticide de-bonding from the surface. Optimization of the pH parameter was important for the point of adsorbent stability, i.e. dissolution of iron ion causing deterioration of the adsorbent surface. Indeed etching of adsorbent surface contributes to small surface area increase which in turn contribute to low adsorption capacity decrease in a subsequent adsorption/desorption cycle. The harmful effect of the acid is reflected in a shorter period of adsorbent used in the application. After performing optimization it was selected that the efficient desorption system: sodium hydrogen carbonate (3%) and salt ( $\text{NaCl}$ , 2%) with the most pronounced financial benefit to be considered in a real process of adsorbent regeneration. The desorption results, after five adsorption-desorption cycles, for Azoxystrobin and Iprodione, showed a low reduction in adsorption efficiency for 14 % and 17 %, respectively. The obtained results indicate that Cell-MG showed moderate adsorption capacity in relation to Azoxystrobin and Iprodione, while on the other hand extraordinary high desorption efficiency without detrimental effect to adsorbent surface indicate on high application capability of Cell-MG hybrid membrane.

### 3.4 Adsorption kinetics

In order to analyze in detail adsorption kinetic the modelling of kinetic data, using different kinetic rate equations: the pseudo-first order (Lagergreen), the pseudo-second order (PSO), i.e. the Ho–McKay model, the second-order rate (Table SI), respectively, applying both linear and non-linear least-squares methods [30]. The best correlation was obtained using non-linear fitting with PSO equation (Table V).

**Tab. V** Pseudo-first, pseudo-second and second order reaction kinetic parameters for the Azoxystrobin and Iprodione adsorption using Cell-MG adsorbent.

Ion/order of kinetic law		Pseudo-first	Pseudo-second	Second order
Azoxystrobin	$q_e$	17.326	35.968	35.968
	$k (k_1, k_2)$	0.015	0.001	0.0008
	$R^2$	0.821	0.999	0.889
Iprodione	$q_e$	29.763	31.045	31.045
	$k (k_1, k_2)$	0.001	0.001	0.0012
	$R^2$	0.714	0.998	0.909

The determination of the PSO rate constants at 25, 35 and 45 °C provide data for determination of activation energy (Eq. (S2)). The obtained value was 14.65 KJ mol<sup>-1</sup> for Azoxystrobin and 11.76 KJ mol<sup>-1</sup> for Iprodione. The obtained results indicate significance of structural characteristics of studied pollutants: geometry/spatial arrangement, dipolarity/polarity and proton donating/accepting properties which contribute to effectiveness of molecule diffusivity and extent of solvent-solute interactions.

Also, the results obtained by fitting the kinetic data with intra-particle Weber–Morris (W-M) (Eq. (S15)), Dunwald-Wagner (D-W) (Eqs. (S16) and (S17)), and Homogenous Solid Diffusion (HSDM) model (Eqs. (S18) and (S19)) was used for evaluation of the overall adsorption kinetics (Table VI).

**Tab. VI** Kinetic parameters of the W-M, D-W and HSDM models for the adsorption of azoxystrobin and iprodione on Cell-MG hybrid membrane.

Intra-particle diffusion	Constants	Azoxystrobin	Iprodione
Weber-Morris (Step 1)	$k_{p1} (\text{mg g}^{-1} \text{min}^{-0.5})$	3.025	2.542
	$C (\text{mg g}^{-1})$	1.285	0.736
	$R^2$	0.986	0.966
Weber-Morris (Step 2)	$k_{p2} (\text{mg g}^{-1} \text{min}^{-0.5})$	0.414	0.486
	$C (\text{mg g}^{-1})$	26.242	20.403
	$R^2$	0.984	0.999
Dunwald-Wagner	$K$	0.007	0.07
	$R^2$	0.960	0.964
Homogenous Solid Diffusion Model	$Ds$	$8.94 \cdot 10^{-12}$	$8.62 \cdot 10^{-12}$
	$R^2$	0.932	0.931

The determination of adsorption rate and evaluation of the rate-limitation step was helped in understanding an overall operative adsorption mechanism. Thus, application of the diffusional rate models was helped in resolving time-dependent change of adsorption effectiveness. Values of intercept  $C (\text{mg g}^{-1})$ , from W-M model fitting, provide data about the boundary layer thickness. The larger intercept means higher boundary layer resistance. In the other word, if the plot passes through the origin the rate-limiting process is only the intra-particle diffusion. Otherwise other rate limitation step, along with intra-particle diffusion, is involved. A high value of W-M constant  $C$  (Table VI) indicates that intra-particle diffusion is not the only rate-limiting step where diffusional processes (external and surface diffusion) control kinetic of the overall process having different contribution in the course of the system equilibration. The value for  $k_{p1}$  shows the fast adsorption rate of the Azoxystrobin and Iprodione are transferred from bulk solution to exterior adsorbent surface and the site easily available with appropriate limitation due to intra-particle diffusion. The value  $k_{p2}$  describes the

part of the process whereby the pesticide travel slowly through the micro- and nano-pores being adsorbed onto liquid/adsorbent interface. According to this both film and intra-particle diffusion governs adsorption process with the prevalence of the latter.

### 3.5 Competitive adsorption study

Nowadays, large demand arises for the effective adsorbent for simultaneous removal of both anions and cations, as well as organic pollutants from natural water. In the course of the analysis of the effectiveness of selected pollutant removal, using synthesized adsorbent, the single-pollutant system was usually used. Otherwise, in order to obtain a realistic picture of the possible use of synthesized adsorbent industrial wastewater or model water containing a mixture of different pollutants is necessary to be used. Therefore, it is important for the applications in practice to examine the adsorption of the individual pollutants under the multi-component systems where the competition between pollutants for the same/similar adsorption sites could be deduced [31].

Competitive adsorption in multi-component system thus undoubtedly define selectivity towards appropriate inorganic/organic pollutants. Due to this, in a subsequent experiments, the adsorption study was performed in a multi-component system, i.e. performing a competitive adsorption study, to evaluate the adsorption selectivity of hybrid adsorbent with respect to a specific pollutant. Such a study offers a comprehensive understanding/difference of an adsorption behavior between single- and multicomponent systems giving exact guidelines for selection/confirmation of the most appropriate adsorbents and related optimal operating condition. Thus, the results of the investigation of Cell-MG hybrid adsorbent for purification of a multi-component system, as it was used mining wastewater [16], is given in Table VII.

**Tab. VII** The competitive removal of anions/cations versus pesticides using Cell-MG membrane from mining wastewater.

Wastewater before treatment		Wastewater after treatment	
pesticide/ions	mg dm <sup>-3</sup>	mg dm <sup>-3</sup>	Removal %
Azoxystrobin	2.2	1.5	31.8
Iprodion	2.6	1.9	26.9
Pb <sup>2+</sup>	3.2	1.8	43.8
Cu <sup>2+</sup>	120.4	92.6	23.1
Ca <sup>2+</sup>	320.3	232	27.6
Mn <sup>2+</sup>	15.1	11.6	23.2
Cd <sup>2+</sup>	5.2	3.1	40.4
Ni <sup>2+</sup>	20.4	13.4	34.3
Zn <sup>2+</sup>	25.3	18.2	28.1
Cr(VI)	0.04	0	100.0
As(V)	16.3	9.4	42.3
SO <sub>4</sub> <sup>2-</sup>	4687.0	4122.1	12.1
Cl <sup>-</sup>	116.7	114.9	1.5

(pH adjusted to ~ 6.1)

Obtained results showed a higher affinity of Cell-MG hybrid adsorbent in relation to certain ions, while lower was found for Azoxystrobin and Iprodione. Adsorption efficiency of anions/cations removal depends on the pollutant nature (ionic radius, electronegativity, etc.),

solution pH, temperature, surface properties of the adsorbent, while additionally the structural characteristics and electron density distribution largely influence adsorption behaviour of pesticide. Thus large interference cause lowering adsorption performance of Cell-MG with respect to a pesticide which indicating that electronic distribution, presented by electrostatic potential, dipolarity/polarity and hydrogen bonding characteristics affect adsorption effectiveness. It means that charged ionic species showed favourable electrostatic attraction with the Cell-MG surface.

A two-component competitive adsorption study was performed to determine adsorption selectivity as an important parameter that defines adsorbent affinity to specific pollutants. Methodology was performed according to literature [32], where separation factor ( $sf$ ), described by Eq. (S20), relative to  $\text{Cu}^{2+}$  ( $sf_i^{\text{Cu}}$ ) was calculated. Obtained  $sf_{\text{Ipr}}^{\text{Cu}}$  and  $sf_{\text{Azo}}^{\text{Cu}}$  values of 2.51 and 3.82 indicate higher affinity of  $\text{Cu}^{2+}$ , while significantly higher values for  $sf_i^{\text{Cd}}$  or  $sf_i^{\text{Ni}}$ , with respect to pesticides, were obtained ( $>4$ ). The low selectivity of Cell-Mg from affinity of magnetite surface to functionalities present at pesticide structure. On the contrary, it was shown that soft heavy metal ions such as  $\text{Pb}^{2+}$ ,  $\text{Cd}^{2+}$  (the hardness, valence state and atomic radius), and oxyanions: As(V) and Cr(VI) showed good affinity/complexation ability to Cell-MG surface [16]. Thus, obtained results suggest that Cell-MG membrane could be used as general-purpose adsorbent considering a real system for waste-water purification.

### 3.6. Analysis of adsorption mechanism: theoretical calculation

From scientific point of view it was further of interest to analyze possible adsorption mechanism taking into account binding modes of pollutant/magnetite surface functionalities using theoretical calculation.

Effective pollutant removal arise from the specific affinity to certain metal ions or organic pollutants to adsorbent surface, i.e. adsorbent surface functionalities. Due to the fact that the adsorption behaviour of most adsorbents follow the surface-controlled mechanisms, the surface structure of adsorbents is significant for consideration of adsorption mechanism. Thus, theoretical studies, using DFT method, provided optimized geometries and Molecular Electrostatic Potential (MEP) maps (Fig. 3) which can help visualize the distribution of electron density and electrostatic potential at the van der Waals surface of studied pesticides. MEP maps provide data on the net point electrostatic effect due to uneven electron density distribution in molecule, and usually correlates well with dipole moments, electronegativity, partial charges and chemical reactivity of the molecule. A three dimensional map of electron density isosurface describe the size, shape, charge density and site of chemical reactivity of the molecules. The values of the electrostatic potential are also given by different colors; red represents regions of most electropositive potential, and it indicates the region of low electron density, i.e. sites favorable for interaction with electrophilic centre; opposite is true for blue region. Quantitative values for different color are also given on Fig. 3. As it can be seen from the MEP maps of the Azoxystrobin and Iprodione, the area with the highest value of negative electrostatic potential are over the electronegative atoms such as atoms O and N. In Azoxystrobin, oxygen atoms from ester group (electrostatic potential at the surface -40.34 kcal/mol and -28.43 kcal/mol), nitrogen atoms from pyrimidine ring (-38.47 kcal/mol and -27.29 kcal/mol) and electron withdrawing cyano group (-28.85 kcal/mol) have the highest negative value of electrostatic potential. In Iprodione, negative electrostatic potential is mostly concentrated at oxygen atom from amide group (-32.87 kcal/mol) and two oxygen atoms from imidazolidine-2,4-dione group (-26.98 kcal/mol and -21.67 kcal/mol). These negative parts of the pesticide molecules can form attractive electrostatic interactions and/or

hydrogen bonds with positive centers from adsorbent surface, mainly protons from hydroxyl groups at magnetite surface.

On the other hand, in Azoxystrobin positive electrostatic potential is mainly concentrated at the hydrogen atoms from cyanophenyl group (from +22.43 kcal/mol to +24.02 kcal/mol) and in Iprodione maximum of positive electrostatic potential is found above and below plane of Imidazolidine-2-4-dione ring (+32.76 kcal/mol). Interestingly, potential around N-H atom from amide group in Iprodione is less positive than expected, only 26, 27 kcal/mol, indicating that this group is the good hydrogen bond donor. Also, two  $\sigma$ -holes from chlorine atoms are detected as the maxima (+10.42 kcal/mol and 9.42 kcal/mol).

These findings are further confirmed by calculating Molecular Interaction Field maps, with hydrogen bond donating and hydrogen bond accepting (HBA) probes (Fig. 4). In Azoxystrobin, two main hydrogen bond accepting sites are lone pairs of ester group (blue lumps at Fig. 4a) and *para*-hydrogen atom from cyanophenyl group can form strong CH/X interactions with electronegative atom lone pair from adsorbent surface (red lump at Fig. 4a). Strongest hydrogen bond accepting sites in Iprodione are oxygen atoms from amide and Imidazolidine-2-4-dione ring while only hydrogen bond donating (HBD) site is CH<sub>2</sub> hydrogen atom from Imidazolidine-2-4-dione ring. Also, MIF calculations have confirmed weak HBD capabilities for NH hydrogen from amide group (energies less than 5 kcal/mol). Both analysis, MEP and MIF, have confirmed that ester oxygen atom from Azoxystrobin will be the best hydrogen bond accepting group in investigated pesticides, thus, it indicates that Azoxystrobin create stronger HBA interactions with hydroxyl groups from magnetite surface.

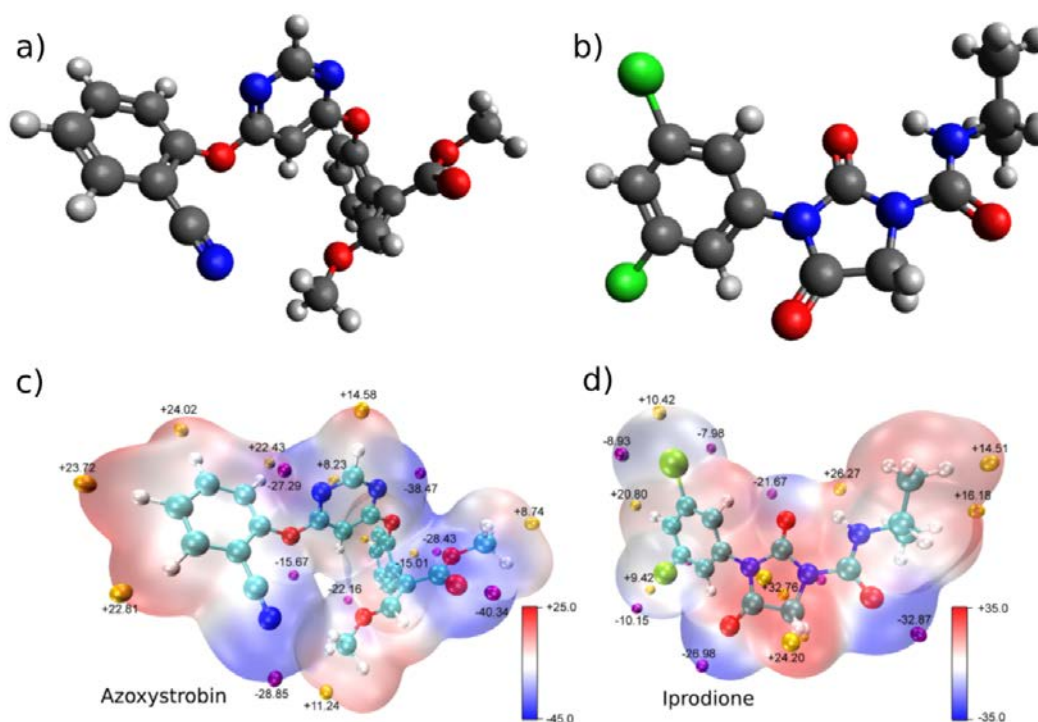


**Fig. 3.** Optimized geometry and Molecular electrostatic potential maps of Azoxystrobin, a) and c), respectively, and Iprodione, b) and d), respectively. The values of local surface minima (purple spheres) and maxima (orange spheres) of electrostatic potential are given in kcal/mol.

From the presented structure and MEP surface it is clear that appropriate electron distribution and spatially oriented HBA/HBD centres provide more favourable arrangement to

establish effective adsorbate/adsorbent surface interactions of Azoxystrobin with hydroxyl group at Cell-MG surface (Fig. 4). On the contrary, geometry of Iprodione and distribution of electronic density indicates less favourable approach to hydroxyl group and thus higher randomness at adsorbent surface was obtained, i.e. higher  $\Delta S^\ominus$  (Tab. IV). The obtained results suggests that electronic density distribution, presented by MEP surface of the studied pesticides, dominantly determine mode of their approach and the binding mechanism with Cell-MG surface functionalities, i.e. dominant electrostatic and HBA interaction. Due to this more favourable interactions could be established at  $\text{pH} < \text{pH}_{\text{PZC}}$ , i.e. with more positive surface, and thus optimal pH 6 was selected for adsorption experiments.

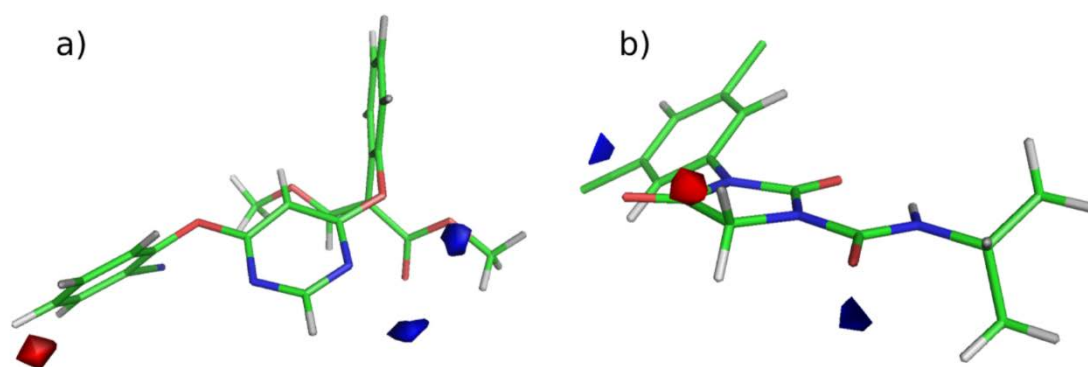


**Fig. 4.** Molecular interaction fields computed for **O** and **N** probe (HBA and HBD probe).

On the Histogram given in Fig. 5 it could be clearly observed somewhat different distribution of electrostatic potential over actual surface area of studied pesticides. Essentially, both effect MEP distribution and structure of the pesticides contribute at different extent to adsorption efficiency. Also, the calculated values of the volume and surface parameters for investigated compounds, given in Table VIII, indicate that obtained higher positive and negative surface area are contributing factor to more intensive interactions of Azoxystrobin with Cell-MG surface. Thus, obtained somewhat better performances, given by adsorption capacity (Table I) and kinetic parameters (Tables V and VI) for Azoxystrobin are valuable results which indicates on appropriate relationship between geometrical/electronic structure of molecules and adsorption performances/bonding mechanism.

**Tab. VIII** Calculated volume and surface parameters for investigated compounds.

Compound	Volume ( $\text{\AA}^3$ )	Surface area ( $\text{\AA}^2$ )	Positive surface area ( $\text{\AA}^2$ )	Negative surface area ( $\text{\AA}^2$ )
Azoxystrobin	476.5	428.9	222.0 (52%)	206.9 (48%)
Iprodione	361.3	336.7	205.7 (61%)	131.0 (39%)

According to presented results it could be supposed that recently synthesized bio-based membrane cross-linked with Cellulose fibres modified with diethylenetriamine (Cell-DETA) and (3-Glycidyoxypropyl)trimethoxysilane (Cell-Glymo), Lignin modified with epichlorohydrine (EL) and Tannic acid (TA) [33] having wealth of the functionalities with different properties (dipolarity/polarity, hydrogen bonding ability, electrostatic interaction etc.) could be more effective adsorbent. Aromatic structure of Azoxystrobin and Iprodione could preferentially interact with large number aromatic structure (from both lignin and tannic acid) able to create  $\pi,\pi$ -interactions with  $\pi$ -electronic density from pesticides. Also, other functionalities, e.g. hydroxyl, phenolic, ether and other, which could create different type of beneficial interactions which may contribute to improved pesticide removal. Further

study will give clear picture on the adsorption potential, except to  $\text{Ni}^{2+}$ ,  $\text{Pb}^{2+}$ ,  $\text{Cr(VI)}$  [31], with respect to pesticides.

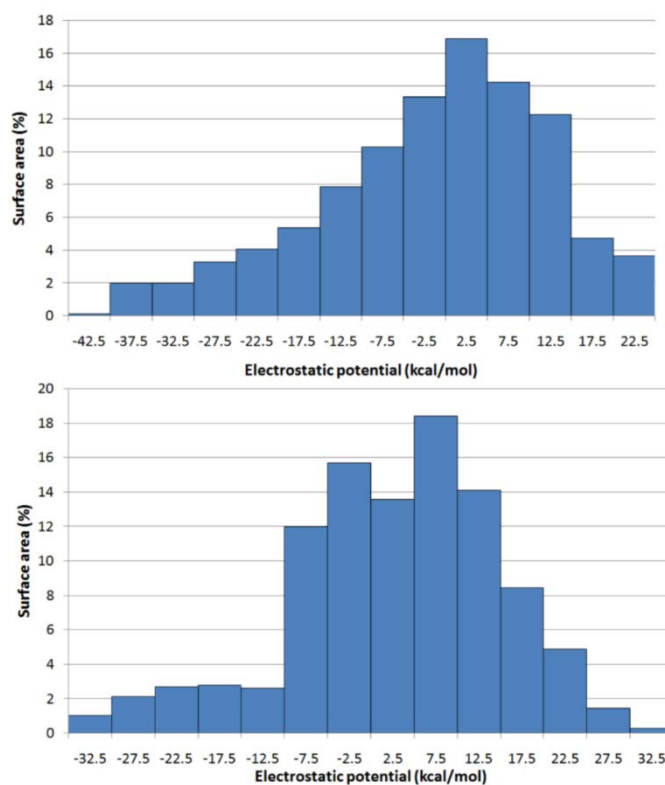


**Fig. 5.** Histogram of surface area versus electrostatic potential for azoxystrobin (top) and iprodione (bottom).

#### 4. Conclusion

In general, the previously synthesized magnetite (MG) modified cross-linked carboxy functionalized cellulose membrane showed moderate effectiveness for Azoxystrobin and Iprodione pesticide removal from water. The moderate adsorption removal from model water, calculated according to non-linear Langmuir model fitting, and wastewater from the mining industry with exceptional high desorption efficiency indicate the moderate performance of Cell-MG membrane for selective pesticide removal. In order to understand mechanism of adsorbate/adsorbent interactions quantum chemical calculations was applied. Obtained results indicate that both factor pesticide geometry and molecular electrostatic surface influences mode and extent of those interactions. The MEP map and MIF results shows that regions with negative potential are over the electronegative oxygen, chlorine and nitrogen atoms, which has a better orientation of the primarily HBA centers in Azoxystrobin for binding with functionalities at Cell-MG surface. On the other hand, the region with positive potential is over the aromatic region which is induced by strong electron-accepting character of hetero atoms. Thus, quantum chemical calculations and experimental results provide deeper insight into influence of the molecular conformation and electronic density distribution on adsorption mechanism. The obtained results and applied methods were in accordance with the current trend in environmental protection where understanding of molecular interaction helps in design new adsorbent with better performances.

## Acknowledgments

The authors acknowledge financial support from Ministry of Education, Science and Technological development of the Republic of Serbia, Contract Nos. 451-03-9/2021-14/200026, 451-03-9/2021-14/200135 and 451-03-9/2021-14/200168).

## 5. References

1. M. Tian, L. Fang, X. Yan, W. Xiao, K.H. Row, *J. Anal. Methods Chem.*, 2019 (2019).
2. A. Sharma, V. Kumar, B. Shahzad, M. Tanveer, G. P. S. Sidhu, N. Handa, S. K. Kohli, P. Yadav, A. S. Bali, R. D. Parihar, O. I. Dar, K. Singh, S. Jasrotia, P. Bakshi, M. Ramakrishnan, S. Kumar, R. Bhardwaj, A. K. Thukral, *SN Appl. Sci.*, 1 (2019) 1-16.
3. A. Mojiri, J. L. Zhou, B. Robinson, A. Ohashi, N. Ozaki, T. Kindaichi, H. Farraji, M. Vakili, *Chemosphere*, 253 (2020) 126646.
4. G. R. Tortella, O. Rubilar, M. Cea, C. Rodríguez-Rodríguez, A. Seguel, J. Parada, *J. Soil Sci. Plant Nutr.*, 19 (2019) 469-476.
5. M. Campos, P.S. Karas, C. Perruchon, E.S. Papadopoulou, V. Christou, U. Menkissoglou-Spiroudi, M.C. Diez, D.G. Karpouzias, *Environ. Sci. Pollut. Res.*, 24 (2017) 152-163.
6. R. K. Ghosh, N. Singh, *J. Agric. Food Chem.*, 57 (2009) 632-636.
7. T. Sumathi, G. Alagumuthu, *Int. J. Chem.Eng.*, 2014 (2014) 1-7.
8. A. E. Burakov, E. V. Galunin, I. V. Burakova, A. E. Kucherova, S. Agarwal, A. G. Tkachev, V.K. Gupta, *Ecotoxicol. Environ. Saf.*, 148 (2018) 702-712.
9. Suhas, V. K. Gupta, P. J. M. Carrott, R. Singh, M. Chaudhary, S. Kushwaha, *Bioresour. Technol.*, 216 (2016) 1066-1076.
10. J. F. Mukerabigwi, S. Lei, L. Fan, H. Wang, S. Luo, X. Ma, J. Qin, X. Huang, Y. Cao, *RSC Adv.*, 6 (2016) 31607-31618.
11. U. Schwertmann, R. M. Cornell, *Iron Oxides in the Laboratory (Second Edition)*, WILEY-VCH Verlag GmbH, Weinheim, 2001.
12. D. Jeremić, L. Andjelković, M. R. Milenković, M. Šuljagić, M.Š. Ristović, S. Ostojić, A.S. Nikolić, P. Vulić, I. Brčeski, V. Pavlović, *Sci. Sinter.*, 52 (2020) 481-490.
13. S. Salazar, D. Guerra, N. Yutronic, P. Jara, *Polymers (Basel)*, 10 (2018).
14. S. S. Stupar, M. M. Vuksanović, L. M. Totovski, R. M. J. Heinemann, D. Ž. Mijin, *Sci. Sinter.*, 53 (2021) 91-117.
15. H. P. Toledo-Jaldin, V. Sánchez-Mendieta, A. Blanco-Flores, G. López-Téllez, A.R. Vilchis-Nestor, O. Martín-Hernández, *Environ. Sci. Pollut. Res.*, 27 (2020) 7872-7885.
16. J. Perendija, Z. S. Veličković, I. Cvijetić, J. D. Rusmirović, V. Ugrinović, A. D. Marinković, A. Onjia, *Cellulose*, 27 (2020) 8215-8235.
17. D. Du, Z. P. Shi, G. Bin Ren, M. H. Qi, Z. Li, X. Y. Xu, *J. Mol. Struct.*, 1189 (2019) 4050.
18. G. W. T. M. J. Frisch, *Gaussian 09 Revision D.01.2013*; Gaussian Inc, Wallingford CT. (2013).
19. T. Lu, F. Chen, *J. Comput. Chem.*, 33 (2012) 580-592.
20. T. Lu, F. Chen, *J. Mol. Graph. Model.*, 38 (2012) 314-323.
21. W. Humphrey, A. Dalke, K. Schulten, *J. Mol. Graphics*, 7855 (1996) 33-38.
22. P. Tosco, T. Balle, *J. Mol. Model.*, 17 (2011) 201-208.
23. A. Munajad, C. Subroto, Suwarno, *Energies*, 11 (2018).
24. C. Ren, X. Ding, W. Li, H. Wu, H. Yang, *J. Chem. Eng. Data*, 62 (2017) 1865-1875.



25. F. Ahangaran, A. Hassanzadeh, S. Nouri, Int. Nano Lett., 3 (2013) 3-7.
26. S. C. Boyatzis, G. Velivasaki, E. Malea, Herit. Sci., 4 (2016) 1-17.
27. S. Armenta, S. Garrigues, M. De La Guardia, Anal. Bioanal. Chem., 387 (2007) 2887-2894.
28. Z. Y. Zhou, X. Kang, Y. Song, S. Chen, Chem. Commun., 48 (2012) 3391-3393.
29. G. D. Vuković, A. D. Marinković, M. Čolić, M. D. Ristić, R. Aleksić, A. A. Perić-Grujić, P. S. Uskoković, Chem. Eng. J., 157 (2010) 238-248.
30. H. Kaygusuz, S. Uzaşçı, F. B. Erim, CLEAN - Soil, Air, Water., 43 (2015) 724-730.
31. J. Hur, J. Shin, J. Yoo, Y. S. Seo, Sci. World J., 2015 (2015).
32. K. Pantić, Z. J. Bajić, Z. S. Veličković, J. Z. Nešić, M. B. Đolić, N. Z. Tomić, A. D. Marinković, Environ. Sci. Pollut. Res., 26 (2019) 24143-24161.
33. J. Perendija, Z. S. Veličković, I. Cvijetić, S. Lević, A. D. Marinković, M. Milošević, A. Onjia, Process Saf. Environ. Prot., 147 (2021) 609-625.

**Сажетак:** Магнетитом (MG) модификована целулозна мембрана (Cell-MG), добијена реакцијом 3-аминосилана и Cell влакана функционализованим дианхидридод диетилентриамин-пентасирћетне киселине (Cell-NH<sub>2</sub> и Cell-DTPA, респективно), коришћена је за уклањање Азоксистробина и Ипродиона из воде. Cell-MG мембрана је структурно и морфолошки окарактерисана употребом ФТ-ИР и ФЕ-СЕМ техника. Утицаји оперативних параметара, тј. *nX*, времена контакта, температуре и масе адсорбента на адсорпцију и кинетику процеса, проучавани су у шаржном систему. Израчунати капацитети од 35,32, односно 30,16 мг г<sup>-1</sup> за Азоксистробин и Ипродион, добијени су применом Ленгмировог модела. Резултати добијени применом Вебер-Морисовог модела указали су да унутарчестична дифузија даје главни допринос укупном отпору транспорта масе. Термодинамички подаци указују на спонтану и ендотермну адсорпцију. На основу вишеструке употребе адсорбента и резултата пречишћавања отпадних вода показано је да се Cell-MG може користити као адсорбент опште намене. Адсорбент/адсорбат површинске интеракције разматране су на основу резултата добијених коришћењем теорије функционала густине (DFT) и израчунавања молекуларног електростатичког потенцијала (MEP). Тако је омогућено боље разумевање односа између адсорпционих перформанси и доприноса неспецифичних и специфичних интеракција у циљу дизајна новог адсорбента са побољшаним својствима.

**Кључне речи:** Целулозна мембрана, магнетит, пестицид, квантно-хемијски прорачуни.

© 2021 Authors. Published by association for ETRAN Society. This article is an open access article distributed under the terms and conditions of the Creative Commons — Attribution 4.0 International license (<https://creativecommons.org/licenses/by/4.0/>).



## Supplementary material

### List of symbols

$C_e$  equilibrium concentration in the solution ( $\text{mg dm}^{-3}$ )

$q_e$  adsorbed amount of pesticide at equilibrium ( $\text{mg g}^{-1}$ )

$q_m$  maximum adsorption capacity ( $\text{mg g}^{-1}$ )

$K_L$  Langmuir constant

$K_F$  Freundlich constant

$n^{-1}$  Freundlich adsorption intensity parameter

$R_L$  dimensionless equilibrium parameter

$C_i$  initial pesticide concentration ( $\text{mg dm}^{-3}$ )

$B$  Dubinin-Radushkevich (D-R) constant ( $\text{mol}^2 \text{kJ}^{-2}$ )

$R$  universal gas constant ( $\text{J mol}^{-1} \text{K}^{-1}$ )

$T$  temperature (K)

$A$  Temkin isotherm equilibrium binding constant ( $\text{dm}^3 \text{g}^{-1}$ )

$b$  Temkin isotherm constant

$\Delta G^0$  Gibbs free energy ( $\text{KJ mol}^{-1}$ )

$\Delta H^0$  enthalpy change of adsorption ( $\text{KJ mol}^{-1}$ )

$\Delta S^0$  entropy change of adsorption ( $\text{KJ mol}^{-1}$ )

$k_1$  pseudo-first rate constant ( $\text{min}^{-1}$ )

$q_t$  adsorption capacity at time  $t$  ( $\text{mg g}^{-1}$ )

$t$  time (min)

$k_2$  the second-order rate constant ( $\text{g mg}^{-1} \text{min}^{-1}$ )

$h_2$  initial sorption rate at  $t \rightarrow 0$  ( $\text{mg g}^{-1} \text{min}^{-1}$ )

$k_i$  intraparticle diffusion rate constant ( $\text{mg g}^{-1} \text{min}^{1/2}$ )

$C_{BL}$  constant related to the thickness of the boundary layer

$K$  rate constant of adsorption ( $\text{min}^{-1}$ )

$D_s$  intraparticle diffusion coefficient

$r$  radial position

## 2. Experimental part

### 2.1 Chemicals and materials

All the chemicals used in this study were of analytical grade and used as received. The stock solutions were prepared with deionized water (DW), resistivity 18 MΩ cm. The pesticide (Azoxystrobin and Iprodione) were kindly provided by company Chemical Agrosava, Serbia. Adjustment of pH was accomplished with 0.1 M NaOH and 0.1 M HNO<sub>3</sub> (Sigma Aldrich).

### 2.2 Cell-MG hybrid membrane preparation

Data on Cell based membrane preparation is given in Supplementary material.

### 2.3 Characterization of adsorbents

#### 2.3.1 FTIR spectroscopy

Fourier-Transfer Infrared Spectroscopy analysis (FTIR) of samples was performed using Thermo Scientific Nicolet 6700 spectrometer in the attenuated total reflectance (ATR) mode. The range of wavenumber was 3500 - 500 cm<sup>-1</sup>.

#### 2.3.2 Surface Morphology analysis

The surface morphology of the samples was examined using a Tescan Mira3 XMU field emission scanning electron microscope (FE-SEM), operated at 20 kV. Microstructural (morphological) characterization was performed on a transmission electron microscope (TEM) JEM-1400.

#### 2.4 Batch adsorption and kinetic experiments

In order to evaluate the performance of the Cell-MG hybrid membrane, batch adsorption experiments were conducted by equilibration of solutions containing azoxystrobin and Iprodione under magnetic stirring. Adsorption experiments were performed by addition of 1, 2, 3, 5, 7.5 and 10 mg of adsorbent in a vials of 9 cm<sup>3</sup> containing 6.1 and 5.1 mg dm<sup>-3</sup> of solutions of Azoxystrobin and Iprodion, respectively. The pH of the solution was adjusted by adding 0.1 M HCl or NaOH aqueous solutions. At predetermined time intervals, approximately 3 cm<sup>3</sup> of pesticide solution were used for UV/Vis measurements and afterwards returned into the vial. This was repeated until equilibrium was reached.

UV-spectrophotometer (SHIMADZU, UV-1700) was used to measure the concentration of pesticide in solution. For the pH measurements a laboratory pH meter, InoLab Cond 730 precision conductivity meter (WTW GmbH), with an accuracy of ± 0.01 pH units, was used. Adsorption equilibrium and thermodynamic parameters were evaluated at three temperatures (25, 35 and 45 °C). The adsorption kinetic was studied by varying the contact time: 1, 5, 15, 30, 60, 90 and 240 minutes at C<sub>i</sub> = 6.1 and 5.1 mg dm<sup>-3</sup> for Azoxystrobin and Iprodione respectively, pH<sub>i</sub> 6 at 25, 35 and 45 °C. After adsorption, the sample solution was filtered through a nylon membrane syringe filter (pore size 0.22 μm). The Azoxystrobin and Iprodione uptake of adsorbent adsorbed per mass unit of the adsorbent were calculated from the Eq. S1:

$$q = \frac{(C_i - C_f)}{m} V \quad (S1)$$

where  $q$  is the adsorption capacity in  $\text{mg g}^{-1}$ ,  $C_i$  and  $C_f$  are the initial and final concentrations of pesticide in the solution in  $\text{mg dm}^{-3}$ ,  $V$  is the volume of solution in  $\text{dm}^{-3}$ , and  $m$  is the mass of the adsorbent in g. Adsorption isotherms are determined as the dependence of  $q$ ,  $\text{mg g}^{-1}$  from equilibrium concentration  $C_e$ ,  $\text{mg dm}^{-3}$  based on the calculated values of  $q$ . Calculated values were fitted to four models of adsorption isotherms (Langmuir, Freundlich, Temkin and Dubinin-Radushkevich models).

Following kinetic results, the Arrhenius equation was employed to describe the temperature dependence of the rate constants and calculate activation energies ( $E_a$ ):

$$k_2 = k_0 \exp\left(-\frac{E_a}{R \cdot T}\right) \quad (\text{S2})$$

where  $k_2$  is the pseudo-second-order rate constant, ( $\text{g mg}^{-1} \text{min}^{-1}$ );  $k_0$  is temperature independent pre-exponential factor, ( $\text{g mmol}^{-1} \text{min}^{-1}$ );  $R$  is the universal gas constant ( $8.314 \text{ J mol}^{-1} \text{ K}^{-1}$ ) and  $T$  is the absolute temperature of adsorption, (K).

The ANOVA variance analysis was used to confirm the validity of the isotherm models by using commercial software OriginPro 9.0. The coefficients  $R^2$ , standard errors ( $SE$ ) for maximum adsorption capacity, Langmuir and Freundlich equilibrium constants, as well as, reduced chi-square analysis ( $\chi_r^2$ ) indicated that the Langmuir isotherm model fits better the experimental results for both materials.

## 2.5 Regeneration study

To evaluate the regeneration capabilities, i.e. desorption capability, after adsorption experiments and washing with DI, wet adsorbents ( $m/V=100 \text{ mg dm}^{-3}$ ) were re-dispersed in  $20 \text{ cm}^3$  of regenerator. Different solution: NaOH (2%, 3% and 4%),  $\text{NaHCO}_3$  (2%, 3% and 4%) and NaCl (2%, 3% and 4%) or their combination was used for pollutant elution. Also, other regenerator  $\text{Na}_2\text{CO}_3$ , KOH, EDTA, *conc.* HCl and sulfuric acid, citric and oxalic acid were used. The amount of desorbed Azoxystrobin and Iprodione was measured after magnetic mixing for 3 h in a batch system. Five consecutive adsorption/desorption cycles were performed in triplicate.

## 2.6. Computational detail

The structure of Azoxystrobin and Iprodione are given in Fig. S1.

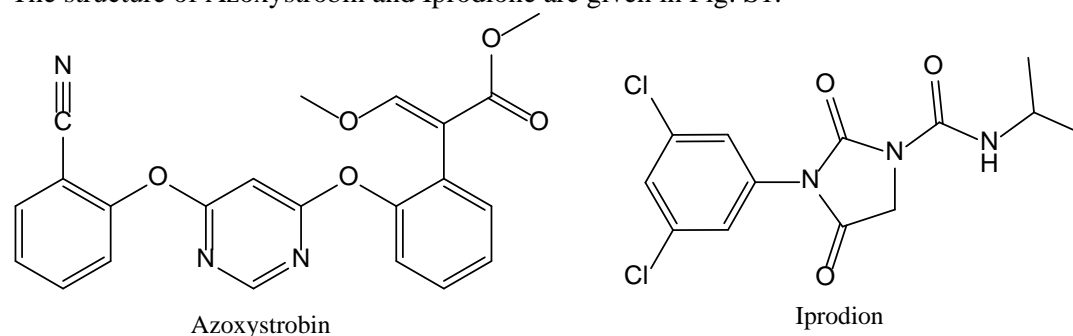


Fig. S1. Molecular structures of Azoxystrobin and Iprodione

### 3. Results and discussion

#### 3.2 Characterization of the adsorbent

##### 3.2.2 Surface Morphology analysis

Surface Morphology analysis of diatomite before and after modification

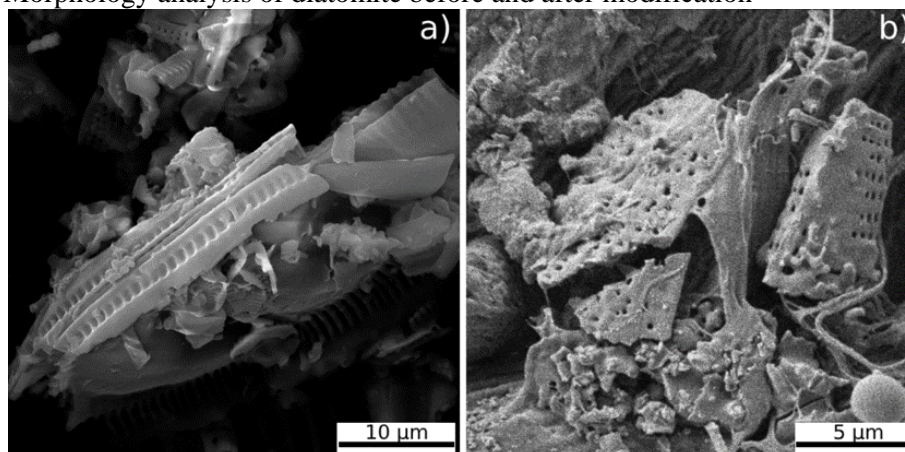


Fig. S2. SEM images of diatomite (a), and D-APTES (b) embedded into Cell-MG matrix

#### 3.3 Adsorption study

##### 3.3.1 Adsorption isotherms modeling

In this study the equilibrium adsorption data were fitted into following isotherm models: Langmuir, Freundlich, Temkin and Dubinin-Radushkevich.

The Langmuir model, Eq. (S3), assumes monolayer adsorption on a homogeneous surface where all sorption sites are found to be identical and energetically equivalent. The Freundlich model, Eq. (S4), assumes the adsorption to be multilayer on a heterogeneous adsorbent surface with a non-uniform distribution of adsorption heat [10].

$$q_e = \frac{q_m K_L C_e}{1 + K_L C_e} \text{ or linear form } \frac{C_e}{q_e} = \frac{1}{K_L q_m} + \frac{C_e}{q_m} \quad (\text{S3})$$

$$q_e = K_F C_e^{\frac{1}{n}} \text{ or linear form } \log q_e = \log K_F + \frac{1}{n} \log C_e \quad (\text{S4})$$

where  $C_e$  is adsorbate concentration in solution at the equilibrium ( $\text{mg dm}^{-3}$ );  $q_e$  is the adsorption capacity at equilibrium ( $\text{mg g}^{-1}$ );  $q_m$  is the maximum adsorption capacity ( $\text{mg g}^{-1}$ ) and  $K_L$  is the Langmuir equilibrium constant ( $\text{dm}^3 \text{mol}^{-1}$ );

The  $K_L$  constant, from Eq. (S3), can be used to calculate a dimensionless equilibrium parameter ( $R_L$ ) by the following equation:

$$R_L = \frac{1}{1 + K_L \cdot C_i} \quad (\text{S5})$$

where  $C_i$  is the highest initial pesticide concentration. Based on  $R_L$  value can be determined the adsorption nature to be either unfavorable ( $R_L > 1$ ), linear ( $R_L = 1$ ), favorable ( $0 < R_L < 1$ ) or irreversible ( $R_L = 0$ ).

In Freundlich equation (Eq. S4)  $K_F$  ( $\text{mg g}^{-1}$ ) ( $\text{dm}^3 \text{mg}^{-1}$ )<sup>1/n</sup> and  $n$  are the Freundlich constants and represent adsorption capacity and adsorption strength, respectively.

The Dubinin-Radushkevich (D-R) isotherm model was used in order to determine if the adsorption occurred by a physical or chemical process. The linear form of this model is expressed by Eq. (S6):

$$\ln q_e = \ln q_m - B(RT)^2 \left[ \ln \left( 1 + \frac{1}{C_e} \right) \right]^2 \quad (\text{S6})$$

where  $B$  ( $\text{mol}^2\text{kJ}^{-2}$ ) and  $q_m$  ( $\text{mg g}^{-1}$ ) are D-R constants, which are calculated from the slope of  $\ln q_e$  versus  $[RT \ln(1 + 1/C_e)]^2$  and intercept.

The Temkin isotherm model implies a uniform distribution of binding energies onto the adsorbent surface and is described by Eq. (S7)[10,11]:

$$q_e = \frac{RT}{b} \ln(AC_e) \text{ or linear form}$$

$$q_e = \frac{RT}{b} \ln A + \frac{RT}{b} \ln C_e \quad (\text{S7})$$

where the  $A$  is the Temkin isotherm equilibrium constant ( $\text{dm}^3 \text{g}^{-1}$ ) and  $b$  is Temkin isotherm constant related to the heat of adsorption.

### 3.3.2 Thermodynamic parameters of adsorption

Gibbs free energy ( $\Delta G^\ominus$ ), enthalpy ( $\Delta H^\ominus$ ) and entropy ( $\Delta S^\ominus$ ) calculated from Van't Hoff equation were used as indicators of the possible nature of adsorption process Eqs. (S8)-(S10):

$$\Delta G^\ominus = -R \cdot T \cdot \ln(K_L) \quad (\text{S8})$$

$$\Delta G^\ominus = \Delta H^\ominus - T \cdot \Delta S^\ominus \quad (\text{S9})$$

$$\ln K_L = \frac{\Delta S^\ominus}{R} - \frac{\Delta H^\ominus}{R \cdot T} \quad (\text{S10})$$

Where  $T$  is absolute temperature (K), and  $R$  is universal gas constant ( $\text{J mol}^{-1}\text{K}^{-1}$ ). Langmuir adsorption constant  $K_L$  is obtained from isothermal experiments.  $\Delta H^\ominus$  and  $\Delta S^\ominus$  are calculated from slopes and interceptions in diagram  $\ln(K_L) - T^{-1}$ , with a premise that the system attained stationary conditions.

### 3.3.3 Desorption studies

To evaluate the regeneration ability of Cell-MG, the exhausted material, obtained after adsorption experiments, were dried at 50 °C for 1 h and used in a desorption study. The material was re-dispersed in DI water and subjected to desorption experiments. The concentration of azoxystrobin and Iprodione in effluent water was measured. After the adsorbent has been regenerated, it was rinsed with DW water and used in subsequent adsorption experiments. The regeneration processes have been investigated by five adsorption/desorption cycles.

The regeneration efficiency, RE in %, was calculated according to Eq. (S11):

$$\text{RE (\%)} = (q_{(i+1)} / q_i) \times 100 \quad (\text{S11})$$

The adsorption capacity of the Cell-MG before and after regeneration step  $q_i$  and  $q_{(i+1)}$  (obtained at the defined condition: adsorbent mass 2.0mg, 7.5 mL of a solution of 10 mg  $\text{dm}^{-3}$  for azoxystrobin and Iprodione and pH 6.5 was used for calculation of RE. Five consecutive adsorption/desorption cycles were performed in triplicate. All collected effluent water was analyzed using UV-Vis spectrophotometer Shimadzu 1800 and HPLC SpectraSystem P4000 with UV1000 detector.

### 3.4 Adsorption kinetics

Kinetic studies provide information about optimum conditions, mechanism of sorption, and possible rate controlling step. In this study pseudo-first, pseudo-second and second order kinetics is applied on experimental adsorption data.

Tab. SI Adsorption kinetic models

Kinetic model	Nonlinear form	Linear form	Equation
pseudo-first order	$q_t = q_e(1 - e^{-k_1t})$	$\ln(q_e - q_t) = \ln q_e - k_1t$	(S11)
pseudo-second order	$q_t = \frac{t}{\frac{1}{k_2q_e^2} + \frac{t}{q_e}}$	$\frac{t}{q_t} = \frac{1}{k_2q_e^2} + \frac{1}{q_e}t$	(S12)
second order	$q_t = \frac{t}{\frac{1}{k_2q_e^2} + \frac{t}{q_e}}$	$\frac{t}{C_t} = k_2t + \frac{1}{C_o}$	(S13)

The pseudo-first order equation (Lagergren rate equation) is often used for the adsorption of an adsorbate from an aqueous solution. The linear form pseudo-first order equation is expressed by the following Eq. S11 [12], where,  $q_t$  (mg g<sup>-1</sup>) is the amount of metal ion adsorbed per unit of adsorbent,  $q_e$  (mg g<sup>-1</sup>) is the adsorption capacity at equilibrium,  $k_1$  (min<sup>-1</sup>) is the pseudo-first order rate constant and  $t$  (min) is the contact time.

The linear form of pseudo-second order model is given by Eq. (S12) [13], where  $k_2$  (g mg<sup>-1</sup> min<sup>-1</sup>) is the pseudo-second order rate constant,  $q_t$  (mg g<sup>-1</sup>) and  $q_e$  (mg g<sup>-1</sup>) are the adsorption capacities. The initial adsorption rate,  $h_2$  (mg g<sup>-1</sup> min<sup>-1</sup>) at  $t \rightarrow 0$  is defined as Eq. (S14):

$$h_2 = k_2q_e^2 \tag{S14}$$

The  $h_2$ ,  $q_e$  and  $k_2$  can be obtained by the linear plot of  $t/q_t$  versus  $t$ .

In this study Weber-Morris, Dunwald-Wagner and Homogeneous solid diffusion model (HSDM) have been used to describe adsorption data.

Weber-Morris model can be used when intra particle diffusion is the only rate-limiting step, because the kinetic data can be well correlated with this model [14]:

$$q_t = k_i t^{1/2} + C_{BL} \tag{S15}$$

Where  $k_i$  (mg g<sup>-1</sup> min<sup>1/2</sup>) is intraparticle diffusion rate constant and  $C_{BL}$  is constant which reflects the boundary layer effect.

Dunwald-Wagner (D-W) is a common equation used to describe intraparticle diffusion [15] D-W relation could be expressed by Eqs. (S16) and (S17):

$$\frac{q_t}{q_e} = 1 - \frac{6}{\pi^2} \sum_{n=1}^{\infty} \frac{1}{n^2} \exp[-n^2 K t] \tag{S16}$$

Where  $K$  (min<sup>-1</sup>) is the rate constant of adsorption. Simplification of the Eq. (S16) gave:

$$\log \left( 1 - \left( \frac{q_t}{q_e} \right)^2 \right) = - \frac{K}{2.303} t \tag{S17}$$

Homogeneous solid diffusion model (HSDM) is a typical intra-particle diffusion model for describe mass transfer in an amorphous and homogeneous sphere [16]. HSDM model can be expressed by differential equation:

$$\frac{\partial q}{\partial t} = \frac{D_s}{r^2} \frac{\partial}{\partial r} \left( r^2 \frac{\partial q}{\partial r} \right) \tag{S18}$$

Where  $D_s$  is intraparticle diffusion coefficient,  $r$  radial position, and  $q$  the time-dependent adsorption capacity. The precisely solution to Eq. (S17) for the defined adsorption condition was given by Crank :

$$\frac{q_t}{q_e} = 1 + \frac{2R}{\pi r} \sum_{n=1}^{\infty} \frac{(-1)^n}{n} \sin \frac{n\pi r}{R} \exp \left[ \frac{-D_s t \pi^2 n^2}{R^2} \right] \tag{S19}$$

The value of  $D_s$  for long-time data can be also determined by plotting of  $\ln(1 - q_t/q_e)$  vs  $t$ .

### 3.5 Competitive adsorption study

The separation factor ( $sf$ ) was quantitatively calculated according to Eq. (S20):

$$sf_i^{Cu} = \frac{q_{e,Cu} C_{e,i}}{q_{e,i} C_{e,Cu}} \tag{S20}$$

where  $C_{e,Cu}$  and  $C_{e,i}$ , as well as  $q_{e,Cd}$  and  $q_{e,i}$  are the equilibrium concentration and capacities of  $Cu^{2+}$  and competitive ion  $i$ , respectively, ( $mmol\ g^{-1}$ ). For dimensionless number  $sf=1$  equal selectivity of  $Cu^{2+}$  and ion  $i$  by adsorbent was obtained, while for  $sf>1$  higher affinity with respect to  $Cu^{2+}$  was obtained. The concentration of ion in collected effluent water was analyzed using atomic absorption spectrometry (AAS) using a Perkin Elmer PinAAcle 900T [17].

## 5. References

- [1] W.C. Griffin, Classification of surface-active agents by "HLB", *J. Soc. Cosmet. Chem.* 1 (1949) 311–326.
- [2] T. Lu, F. Chen, *J. Comput. Chem.*, 33 (2012) 580–592.
- [3] J.J.P. Stewart, *J. Mol. Model.*, 19 (2013) 1–32.
- [4] James J. P. Stewart, *J. Comput. Aided. Mol. Des.*, 4 (1990) 1–103.
- [5] H.B.S. et al. M. J. Frisch, G. W. Trucks, Gaussian 16 Revision B. 01. 2016; Gaussian Inc, Wallingford CT. 46 (2016).
- [6] W. Humphrey, A. Dalke, K. Schulten, VMD : Visual Molecular Dynamics, 7855 (1996) 33–38.
- [7] A. Pedretti, L. Villa, G. Vistoli, VEGA – An open platform to develop chemo-bio-informatics applications, using plug-in architecture and script programming, (2004) 167–173.
- [8] P.J. Goodford, *J. Med. Chem.*, 28 (1985) 849–857.
- [9] M. Pastor, G. Cruciani, I. Mclay, S. Pickett, S. Clementi, GRid-INdependent Descriptors ( GRIND ): A Novel Class of Alignment-Independent Three-Dimensional Molecular Descriptors, (2000) 3233–3243.
- [10] K.Y. Foo, B.H. Hameed, *Chem. Eng. J.*, 156 (2010) 2–10.
- [11] M. Karanac, M. Đolić, Đ. Veljović, V. Rajaković-Ognjanović, Z. Veličković, V. Pavićević, A. Marinković, *Waste Manag.*, 78 (2018) 366–378.
- [12] H. Moussout, H. Ahlafi, M. Aazza, H. Maghat, *Karbala Int. J. Mod. Sci.*, 4 (2018) 244–254.
- [13] Z. Ren, G. Zhang, J. Paul Chen, *J. Colloid Interface Sci.*, 358 (2011) 230–237.
- [14] L. Soldatkina, M. Zavrishko, *Colloids and Interfaces.*, 3 (2018) 4.
- [15] H. Qiu, L. Lv, B.C. Pan, Q.J. Zhang, W.M. Zhang, Q.X. Zhang, *J. Zhejiang Univ. Sci. A.* 10 (2009) 716–724.
- [16] R.M.C. Viegas, M. Campinas, H. Costa, M.J. Rosa, *Adsorption.*, 20 (2014) 737–746.
- [17] J. Perendija, Z.S. Veličković, I. Cvijetić, J.D. Rusmirović, V. Ugrinović, A.D. Marinković, A. Onjia, *Cellulose.*, 27 (2020) 8215–8235.